Published in final edited form as:
Neuron. 2013 May 22; 78(4): 658–672. doi:10.1016/j.neuron.2013.03.019.

The ventral hippocampus is the embryonic origin for adult neural stem cells in the dentate gyrus

Guangnan Li[1,*], **Li Fang**[2], **Gloria Fernández**[1], and **Samuel J. Pleasure**[1,*]

[1]Department of Neurology, Programs in Neuroscience and Developmental Stem Cell Biology, Institute for Regenerative Medicine, University of California, San Francisco, CA 94158

[2]Epitomics - an Abcam Company, 863 Mitten Road, Suite 103, Burlingame, CA 94010

SUMMARY

Adult neurogenesis represents a unique form of plasticity in the dentate gyrus requiring the presence of long-lived neural stem cells (LL-NSCs). However, the embryonic origin of these LL-NSCs remains unclear. The prevailing model assumes that the dentate neuroepithelium throughout the longitudinal axis of the hippocampus generates both the LL-NSCs and embryonically produced granule neurons. Here we show that the NSCs initially originate from the ventral hippocampus during late gestation and then relocate into the dorsal hippocampus. The descendants of these cells are the source for the LL-NSCs in the subgranular zone (SGZ). Furthermore, we show that the origin of these cells and their maintenance in the dentate are controlled by distinct sources of Sonic Hedgehog (Shh). The revelation of the complexity of both the embryonic origin of hippocampal LL-NSCs and the sources of Shh has important implications for the functions of LL-NSCs in the adult hippocampus.

INTRODUCTION

There are two sites of adult neurogenesis in the rodent central nervous system (CNS): the cortical subventricular zone (SVZ) and the dentate subgranular zone (SGZ) in the hippocampal formation. In the dentate gyrus (DG), adult neurogenesis refines network functions by constant addition of new neurons to the granule cell layer (GCL) (Clelland et al., 2009; Li and Pleasure, 2010; Sahay et al., 2011). However, little is known about the developmental program controlling the formation of the neurogenic niche where neurogenesis is sustained in the DG (Altman and Das, 1967). Compared to the SVZ, the most pronounced feature of DG niche development is the complete dissociation of the long-lived neural stem cells (LL-NSCs) in the SGZ from the embryonic germinative zone (Altman and Bayer, 1990a; Li et al., 2009).

Previous studies presumed that the LL-NSCs in the SGZ arise from the neuroepithelium adjacent to the cortical hem during embryonic development of the hippocampus (Li and Pleasure, 2005), either directly translocating from the VZ to the dentate primordium (Eckenhoff and Rakic, 1984) or indirectly relocating from the migratory stream formed

*Correspondence: grant.li@ucsf.edu (G.L.), sam.pleasure@ucsf.edu (S.J.P.).

Author Contributions: G.L. conceived of and performed the experiments, analyzed the data and wrote the manuscript. L.F. and G.F. performed experiments and analyzed data. S.P. conceived of experiments, analyzed data and wrote the manuscript.

during late gestation (Altman and Bayer, 1990a). This model is somewhat supported by the analysis of mutants either defective in cortical hem development or in the reception of key signals from the cortical hem. The cortical hem is a hippocampal organizer enriched in signaling molecules (such as Wnts and Bmps) that patterns the hippocampal neuroepithelium into functionally distinct subfields (Mangale et al., 2008), including the primordium of the DG. The loss of the transcription factor Lef1, a mediator of the canonical Wnt signaling pathway, results in the underproduction of granule cells perinatally (Galceran et al., 2000; Zhou et al., 2004) and complete loss of the SGZ postnatally (Li et al., 2008). Meanwhile, ectopic upregulation of canonical Wnt signaling in the hippocampal neuroepithelium is sufficient to promote granule cell fate (Machon et al., 2007). These studies provide evidence that Wnt activity is critical for promoting granule cell fate prenatally. However, direct evidence supporting that SGZ LL-NSCs originate from the equivalent septotemporal level of the dentate neuroepithelium is still missing.

Recently, it has become clear that the Hedgehog (Hh) signaling pathway is prominently involved in SGZ development. The ablation of Smo, the obligatory receptor for Hh signaling (Machold et al., 2003), or the impairment of primary cilia, an organelle essential for Hh signaling (Breunig et al., 2008; Han et al., 2008), leads to SGZ deficiency but apparently still allows production of granule neurons at embryonic stages. Fate mapping analysis also reveals that embryonic dentate NSCs are Hh-responsive during late gestation before they populate their permanent niche in the dentate and that quiescent SGZ NSCs are still Hh-responsive throughout adulthood (Ahn and Joyner, 2005; Encinas et al., 2011). What is not clear from these studies is whether precursors in the embryonic dentate VZ are the Hh-responding cells and how the Hh-responding NSCs interact with the Hh-producing cells during relocation.

In this study we set out to determine how Hh signaling controls the formation of the dentate SGZ by investigating when and where NSCs perceive Hh ligands before ultimately settling in the SGZ, and more importantly, to explore the germinative origins of LL-NSCs. We find that SGZ formation requires an extra-cortical source of Hh during late embryonic stages. More intriguingly, the ventral hippocampus is the main cellular source for the SGZ. Long-term fate mapping analysis further confirms that the prenatal Hh-responding cells restricted in the amygdalo-hippocampal region contribute to the LL-NSCs of the SGZ. In contrast to long-held assumptions in the literature, these observations lead to a new model that the LL-NSCs from the ventral hippocampus migrate along the longitudinal axis of the hippocampus from temporal to septal poles before settling. Subsequently, local neuronal sources of Shh maintain these LL-NSCs in the SGZ postnatally and throughout adulthood. The results of our study support the idea that the adult dentate gyrus is a mosaic structure. The embryonically produced DGCs from equivalent anatomic levels of the dentate in the septotemporal plane are supplemented by the DGCs whose progenitors originate from the most caudotemporal region of the ventral hippocampus. This raises new questions about the nature of the granule neuron heterogeneity and the regulation of neurogenesis.

RESULTS

Hh-responsive cells are concentrated in the ventral hippocampal neuroepithelium during late gestation

Previous studies reported that during the last week of gestation in rodents, a migratory stream from the dentate neuroepithelium adjacent to the cortical hem courses through the fimbriodentate junction (FDJ) and either assumes a subpial route or fans out into the hilus (Altman and Bayer, 1990a; Li et al., 2009). Prospective NSCs destined for the SGZ are believed to derive from this migratory stream (Altman and Bayer, 1990a) or directly translocate from the dentate primordium (Eckenhoff and Rakic, 1984). Taking into

consideration the findings that NSCs responding to Hh can be labeled during late gestation (Ahn and Joyner, 2005; Li et al., 2009) and that Hh-signaling is required to establish SGZ progenitors (Han et al., 2008; Machold et al., 2003), we reasoned that upon perceiving Hh in the dentate VZ or along the migratory stream, precursors are induced or specified to become dentate NSCs. To test this hypothesis, we decided to begin with the Hh-responding line Gli1-nLacZ (Bai et al., 2002) to study the static distribution of Hh-responding cells at the perinatal ages when the prospective SGZ NSCs can be traced by the tamoxifen inducible line Gli1-CreERT2 (Ahn and Joyner, 2005; Li et al., 2009).

The rodent hippocampus is situated at the mediotemporal edge of the neocortex and straddles the thalamus along its septotemporal axis. Dorsal to the thalamus is the dorsal hippocampus whereas ventral to the thalamus is the ventral hippocampus. Sagittal sections at different mediolateral levels (shown as schemas in Figure 1a and e) allow us to comprehensively examine the distribution of Gli1-nLacZ+ cells throughout the developing hippocampus including both the dorsal and ventral arms.

To our surprise, at E17.5 Gli1-nLacZ+ cells were basically absent from the dorsal dentate primordium (arrowheads in Figure 1b′, c′). By contrast, Gli1-nLacZ expression occupied the whole VZ of the ventral hippocampus at the far end of the temporal pole (arrowhead in Figure 1b″), about half at the mid-level (arrowhead in Figure 1c″), but only about one-third at the transitional level (arrowhead in Figure 1d′). At the most temporal level, Gli1-nLacZ+ cells were noticeably distributed from VZ to the forming DG (arrow in Figure 1b″).

By P0, Gli1-nLacZ remained absent from the dorsal dentate primordium (arrowheads in Figure 1f′, g′), and only sparse Gli1-nLacZ+ cells were detectable in the dorsal DG (arrows in Figure 1f′ and g′). However, Gli1-nLacZ expression now covered the whole VZ of the ventral hippocampus at all levels (arrowheads in Figure 1f″, g″ and h′). Gli1-nLacZ+ cells were observed in the ventral forming DG at the more lateral/septal level (arrows in Figure 1g″). At the transitional level, Gli1-nLacZ+ cells were distributed from the ventral to the dorsal arm around the fimbria (arrows in Figure 1h′). The perinatal distribution of Hh-responding cells in the hippocampus prompted us to investigate whether the descendants of these perinatal Hh-responding cells, when most of them are still restricted in the ventral hippocampus by birth, give rise to the NSCs that settle in the SGZ at all septotemporal levels.

Postnatal fate-mapping analysis of cells responding to Hh at prenatal and perinatal ages

In our previous study, we showed that some derivatives of the Hh-responding cells labeled at E17.5 constituted the postnatal radial glia in the SGZ of the DG (Li et al., 2009). In light of our new finding that Gli1-nLacZ+ cells mostly populated the VZ of the ventral hippocampus at this age, we wished to know how these cells contribute to the dentate gyrus at all septotemporal levels. To address these questions, we turned to fate mapping analysis using the Gli1-CreERT2 line (Ahn and Joyner, 2004) crossed to the cre reporter line Ai14 (Rosa-CAG-LSL-tdTomato-WPRE) (Madisen et al., 2010). After independent tamoxifen injections at E15.5, E17.5 or P0, the distribution of recombined cells was examined at P15 (Figure 2a–i). If the recombined cells generate the NSCs eventually located in the SGZ, we expected that radial NSCs and clusters of granule cells (the progeny of the NSCs) would be labeled by tdTomato (tdT) expression by this age.

When tamoxifen was injected at E15.5, a small number of tdT+ clusters were found in the suprapyramidal blade of the ventral DG (arrowhead in Figure 2a), whereas very few isolated tdT+ cells were seen in the transitional ventral DG (arrow in Figure 2b) and in the dorsal DG (arrows in Figure 2c). When tamoxifen was injected at E17.5, tdT+ clusters were found in the DG at all the septotemporal levels (Figure 2d–f). At the current dosage of tamoxifen

(3mg/40g animal), 69±4% of the Blbp+ cells displaying radial orientation in the SGZ were also tdT+ at P15 (Figure S1b, b′ and c), whereas 61±6% of the Sox2+ cells were also tdT+ (Figure S1a, a′ and c). The pattern of tdT+ clusters labeled at E15.5 showed minimal overlap with those labeled at E17.5, indicating that the effect of tamoxifen was transient and diminished by 48hrs. When tamoxifen was injected at P0, tdT+ clusters were found in the inner aspect of the GCL in the ventral DG (arrowheads in Figure 2g–h, the arrow in Figure 2h indicated the boundary between ventral and dorsal DG). Meanwhile, tdT+ clusters continued to heavily make up the dorsal DG at all levels (Figure 2i). Therefore, the Hh-responding cells in the ventral hippocampus start to make a large contribution to the ventral DG around E15.5 and to the dorsal DG around E17.5.

Progeny of Hh-responding cells from the temporal pole arrive in the dentate septal pole ahead of the appearance of local Hh-responding cells

Static analysis showed that Gli1-nLacZ+ cells were initially concentrated in the ventral hippocampus and then later appeared in the developing DG in a temporal(high)-to-septal(low) gradient. We define these two populations as early Hh-responding cells in the VZ of ventral hippocampus, and late Hh-responding cells in the local DG, respectively. The expression of Gli1-nLacZ in the late Hh-responding cells might be due either to the retention of the LacZ protein after they leave their origin or to actively responding to local Shh after they reach the forming DG. We wished to determine the spatial relationship of the progeny of early Hh-responding cells relative to the late Hh-responding cells in the developing DG at birth. To address this, we examined the progeny of the Hh-responding cells marked by tamoxifen injection at E17.5 after crossing the Gli1-CreERT2 line with Ai14 in the mice also carrying Gli1-nLacZ to identify late Hh-responding cells at the same time points and anatomic levels. At P0, we examined the expression of both tdT and LacZ using alternate sagittal sections covering all septotemporal dentate levels (the complete data set is in Figure S1d). X-gal staining rather than antibody staining was used to maximize the detection sensitivity for LacZ. Interestingly, at more temporal levels, tdT+ cells (Figure 2m) had a wider distribution than Gli1-nLacZ+ cells (Figure 2j). At more septal levels, tdT+ cells were still present (arrows in Figure 2n, 2n′, 2o, 2o′), whereas nLacZ+ cells were scarce (Figure 2k) or completely absent (Figure 2l) from the dentate plate, despite the presence of nLacZ+ cells in the meninges labeled by Laminin (presumed to be meningeal fibroblasts) (Figure 2m). These results demonstrated that progeny marked at E17.5 with the Gli1-CreERT2 line can reach more septal levels before late Hh-responding cells are established locally at the same septotemporal levels in the developing DG.

The descendants of the Hh-responding cells from the ventral hippocampal VZ display a continuous stream into the dorsal DG

The above data inspired us to determine the spatial connection between the progeny of the Hh-responding cells and the ventral hippocampal VZ. To do this, we initially analyzed the distribution of tdT+ cells one day after tamoxifen induction at E16.5 (Figure 3a–f). We confirmed that heavy recombination indeed occurred in the VZ of temporal hippocampus (oval in Figure 3b) but was completely absent from the VZ of the dorsal dentate (arrowhead in Figure 3c). From temporal to septal hippocampus (arrows in Figure 3b->e->f->c), the gradient distribution of tdT+ closely mimicked the pattern of Gli1-nLacZ+ cells at the similar age (Figure 1b–c).

Then we analyzed the representative sagittal levels (Figure 3g–i) and the serial sagittal sections (Figure S2) for the distribution of tdT+ cells at P0 with tamoxifen induction at E17.5. The tdT+ cells formed a continuous stream (arrows in Figure 3g′) from the VZ at the temporal pole of the ventral hippocampus (white oval in Figure 3g′) to the forming ventral dentate GCL, which showed close apposition to the meninges at the ventral fimbriodentate

junction (vFDJ) (Figure 3g, g′). Of note, the tdT+ cells seen in the mantle of the amygdalo-hippocampal region could have arisen from the amygdalo-hippocampal VZ (oval in Figure 3g′). At the mediolateral level where the dorsal and ventral dentate gyri joined each other (green oval in Figure 3h, h′), a large number of tdT+ cells were apparent. The higher cell density in this region probably indicated ongoing local proliferation. In the dorsal hippocampus, most tdT+ cells localized in the dorsal fimbriodentate junction (dFDJ) (green oval in Figure 3i, i′), and some of them were distributed further into the hilus at the same longitudinal levels (Figure 3i′). The presence of the tdT+ cells near the upper blade indicated there might be *de novo* induction of Hh-responding cells (Figure 3i′). Quite strikingly, the tdT+ cells at the dFDJ had little connection to the dorsal dentate neuroepithelium at any levels and this cell population likely represented the “intrinsic component” first described by Altman et al. (Altman and Bayer, 1990a). All these data taken together reinforce our new model (Figure 3j) that the progeny of the Hh-responding cells from the ventral hippocampus VZ feed into the dentate gyrus during late gestation in the temporoseptal direction (red arrow in Figure 3j), initially staying in the vFDJ/dFDJ close to the meninges and then radiating into the hilus before the SGZ forms.

Hh-responding cells in the hippocampus of Hh signaling mutants

What is the anatomic Shh source for the Hh-responding cells in the VZ of the ventral hippocampus? Previous studies suggested that Shh from the subpallial septum might regulate NSCs in the adult DG through the long-range axonal targeting via the septohippocampal pathway (Lai et al., 2003). However, it is not clear whether Shh from the septum would regulate the developing DG, particularly at these ages when the septohippocampal projection is not yet fully developed (Super and Soriano, 1994). In order to pinpoint the Hh-producing cells that interact with the dentate precursors, we compared the distribution of the Hh-responding cells around birth between Emx1cre-Shh and Emx1cre-Smo conditional mutants. If other Hh members (Dhh or Ihh) within the Emx1 domain or Hh sources (Shh or other members) outside the Emx1 domain (essentially the dorsal forebrain) were required for the development of the DG, Hh-responding cells would be expected to be unaffected in the Emx1cre-Shh cKO.

By crossing Emx1cre to the cre reporter Rosa-Yfp, we confirmed that at P1 Emx1-cre showed recombination in the ventral hippocampus (Figure 4b), including its VZ (Figure S3b and b′). By P1, Gli1-nLacZ+ cells were found in the dorsal DG of the wild type control (Figure 4c) but mostly absent from the Emx1-Shh cKO at the same anatomical level (Figure 4e). When one copy of the Gli1-nLacZ was present, Gli1-nLacZ+ cells were completely abolished throughout the DG along the whole longitudinal axis in both Emx1-Shh and Emx1-Smo cKOs (Figure 4e, f, g and h). However, the Gli1-nLacZ+ cells in the VZ of the ventral hippocampus were entirely missing only in Emx1-Smo mutants (arrowheads in Figure 4h′) not Emx1-Shh mutants (arrowheads in Figure 4f′), even though they were not as abundant as in the control (arrowheads in Figure 4d′). In the Emx1-Shh cKO, Gli1-nLacZ+ cells (likely due to the slow turnover of nLacZ) were also detected in a region slightly away from the VZ of the ventral hippocampus (arrows in Figure 4f′), as in the control (arrows in Figure 4d′).

It has been reported that Gli1-nLacZ expression is affected by the functional copy number of Shh (Garcia et al., 2010). We reasoned that different copy numbers of Shh and Gli1-nLacZ would give us further insights into the formation of Gli1-nLacZ+ cell stream from the VZ of the ventral hippocampus and the *de novo* induction of Hh-responding cells in the forming DG. To facilitate the analysis, the developing dorsal dentate can be divided into upper and lower portions by a line connecting the tip of the CA3 field and the apex of the dentate pole. In relation to the $Gli1^{Z/+};Shh^{F/F}$ animals (Figure S3d, d′, e, e′), when one copy of the Shh flox allele was replaced with a Shh null allele in the $Gli1^{Z/+};Shh^{F/-}$ animals, the number of

Gli1-nLacZ+ cells in the dorsal dentate was dramatically reduced in both portions (Figure S3f, f′), the Gli1-nLacZ expression showed a decreased level in the VZ of the ventral hippocampus and the stream of the Gli1-nLacZ+ cells emanating from the VZ was also reduced (Figure S3g, g′). Interestingly, all of these phenotypes could be restored in the $Gli1^{Z/Z};Shh^{F/-}$ animals when an extra copy of Gli1-nLacZ was present (Figure S3h, h′, i and i′). However, when the remaining Shh flox allele was floxed out in the Emx1 domain in the $Emx1^{cre/+};Gli1^{Z/Z};Shh^{F/-}$ animals, most of the Gli1-nLacZ+ cells were abolished in the upper portion of the dorsal dentate whereas residual Gli1-nLacZ+ cells were still present at the entrance of the hilus in the lower portion (Figure S3j, j′), which appeared to be continuous with the Gli1-nLacZ+ cell stream from the VZ of the ventral hippocampus (Figure S3k, k′). The Gli1-nLacZ distribution pattern in the $Emx1^{cre/+};Gli1^{Z/Z};Shh^{F/-}$ animals was phenocopied in the $Neurod6^{cre/+};Gli1^{Z/+};Shh^{F/F}$ animals when two copies of the Shh floxed allele were removed from the pallial neuronal lineage (Goebbels et al., 2006) (Figure S3l, l′, m and m′) but not the ventral hippocampal VZ (Figure S3c, c′). Therefore, Shh from the neuronal cells within the Emx1 domain contributes to the *de novo* Hh-responding activity seen locally in the DG, whereas Hh from outside the Emx1 domain is responsible for the Hh-responding activity in the VZ of the ventral hippocampus in the $Emx1^{cre/+};Gli1^{Z/Z};Shh^{F/-}$ animals.

This somewhat unexpected finding led us to ask whether Shh was the only Hh family member responsible for the Hh-responding activity in the amygdalo-hippocampal region. We used the CNS-specific cre (NesCre) to conditionally remove Shh. The NesCre-Shh conditional mutants showed complete absence of Hh-responding cells in both DG (Figure 4i) and the VZ of the ventral hippocampus (Figure 4j, j′). The CA fields in the ventral hippocampus also showed a distorted appearance due to the development of hydrocephalus and/or patterning defects in the NesCre-Shh conditional mutant (Figure 4j and data not shown). Therefore, we conclude that Shh is the sole ligand required for Hh-responding cells in the ventral hippocampus but that Shh is produced by both a local source for the forming DG and an extracortical source for the VZ of the ventral hippocampus.

Crossing Shh-Gfpcre mice with Ai14 allowing cumulative fate mapping for Shh expressing cells revealed that a domain of tdT+ cells was localized within the amygdala, close to the ventral hippocampus (arrow in Figure 4k). By crossing the tamoxifen inducible Shh-CreERT2 line with Ai14, a subset of tdT+ were found in the same amygdalar domain when the expression was examined at P1 after tamoxifen injection at E17.5 (Figure 4l), suggesting that amygdalar Shh was actively expressed at E17.5. This is in line with the Shh mRNA expression pattern in the Allen Brain Atlas Database (http://developingmouse.brain-map.org/data/search/gene/index.html?term=shh). These tdT+ cells coexpressed the transcription factor Nr2f2 (displaying high level of expression in the amygdala) (arrows in Figure 4m), but were excluded from the Otp domain (Figure 4l). The timing and location of the Shh expression in the amygdala suggested that it is a likely Shh source regulating the Hh-responding cells in the ventral hippocampus.

Shh signaling conditional mutants support a complex anatomical origin for dentate stem cells

The analysis above showed that all the Hh-responding activity was abolished in both the hilar region and the VZ of the ventral hippocampus in the Emx1-Smo cKOs, whereas in the Emx1-Shh cKOs Hh-responding activity was eliminated only in the hilar region but was still present in the VZ of the ventral hippocampus. We wished to further examine the migratory streams of the developing DG in the Emx1-Shh cKOs and Emx1-Smo cKOs with the generic proliferation marker Ki67 (Figure 5a–g) and neurogenic precursor marker Tbr2 (Figure 5h–n).

The removal of the obligatory Hh co-receptor Smo from the pallial region by Emx1-cre resulted in a severe reduction of Ki67+ cell density by 75±2% in the hilar region at the transitional level of the DG (arrows in Figure 5b) in relation to the control (arrows in Figure 5a). However, the removal of Shh by the same cre driver only led to a moderate proliferation decrease by 22±5% (arrows in Figure 5c). Noticeably, compared to the control (arrowheads in Figure 5a), Ki67+ cells at the entrance of hilus from the ventral hippocampus were more affected in the Emx1-Smo cKO (arrowheads in Figure 5b) than the Emx1-Shh cKO (arrowheads in Figure 5c). Similarly, Ki67+ and Tbr2+ cells in the dorsal FDJ were significantly diminished by 71±2% and 63±3%, respectively, in the Emx1-Smo cKO (arrows in Figure 5e, i) but only slightly decreased by 19±5% and 3±5%, respectively, in the Emx1-Shh cKO (arrows in Figure 5f, j), as compared to the control (arrows in Figure 5d, h). In contrast, the dorsal SVZ of the dentate was minimally affected in both Emx1-Smo and Emx1-Shh cKOs, as judged by Ki67 and Tbr2 (arrowheads in Figure 5d–f and h–j, respectively). Tbr2+ cells in the migratory stream of the ventral hippocampus were also reduced by 55±3% in the Emx1-Smo cKO but had little change (104±3% over the control) in the Emx1-Shh cKO (arrows in Figure 5k–m). All these data strengthen the model that progeny of the Hh-responding cells from the VZ of the ventral hippocampus serve as the critical source for the cells migrating into the dorsal DG, and a Shh source outside the Emx1 domain essentially controls the size of this stream whereas the role of local Shh source in the DG is dispensable for this process.

Shh sources for the postnatal dentate gyrus

The cumulative fate mapping analysis with the Shh-gfpcre line (Harfe et al., 2004) showed complex dynamics of distribution for the Shh-lineage in the developing DG. Some of the cells derived from the Shh lineage were oligodendrocyte progenitors in the prenatal and perinatal DG (Figure S4a–c). However, conditional mutant mice deleting Shh from the oligodendrocyte lineage with Olig2-cre (Schuller et al., 2008) had very little alteration to the Hh-responding cells in the DG as examined at P7 (Figure S4d). The Shh-lineage was fate-mapped postnatally to the hilar mossy cells, as defined by Calretinin+ staining in the dorsal DG (Figure 6a, a′, a″) but not the ventral DG (Figure 6b, b′, b″). Mossy cells derived from the Shh lineage projected to the inner molecular layer of the DG (Figure 6a, a″). In addition, neurons in the medial entorhinal cortex (MEC) (Figure S4e–g), which project to the middle molecular layer of the DG (Figure 6a″, b″), were also part of the Shh lineage.

In order to evaluate the contribution of neuronal (mossy cells and/or MEC) Shh to the Hh-responding activity in the postnatal DG, the distribution of Gli1-nLacZ+ cells was examined at P7 in the mutant mice in which Shh was conditionally removed from the neocortical and hippocampal neurons by Neurod6-cre (Goebbels et al., 2006). Compared to the control (Figure 6c, f), the loss of Hh-responding activity in the hilus of Neurod6-Shh cKO (Figure 6e, h) was almost as effective as Emx1-Shh cKO (Figure 6d, g). Therefore, the neuronal Shh is the key source responsible for the Hh-responding activity locally in the DG.

The role of the local Shh in SGZ formation and maintenance

Our data favors the new model that ventral hippocampus-derived NSCs contribute to the NSCs in the SGZ. However, if the local Shh plays a critical role in the formation of the SGZ, its absence would result in severe SGZ deficiency. To test this, we looked into SGZ formation at P15 by removing either Smo or Shh from the hippocampus with Emx1-cre and compared their phenotypes for SGZ formation. In relation to the control (Figure 7a), there was a complete lack of the radial glia marker Blbp in the SGZ of Emx1-Smo cKO (Figure 7b) but only a mild decrease of the Blbp cell density by 28±4% in the SGZ of Emx1-Shh cKO (Figure 7c, i) and 18±3% in Neurod6-Shh cKO (Figure 7d, i). Consistently, the radial glial scaffolding in the DG, visualized by Gfap staining, was severely affected in the Emx1-

Smo cKO but relatively intact in the Emx1-Shh cKO and Neurod6-Shh cKO (Figure S5a–d, a′–d′). In addition, we examined the length of the two blades of the dentate gyrus among these mutants. In comparison with the control, the length of the upper and lower blades were 61±1% and 24±1% in the Emx1-Smo cKO, whereas they were 81±5% and 76±3% in the Emx1-Shh cKO, and 102±4% and 98±3% in the Neurod6-Shh cKO (Figure S5e). Compared to the complete absence of proliferation in the SGZ of Emx1-Smo cKO (Figure 7f, Figure S5g, g′), there was a relatively milder proliferation defect in the Emx1-Shh cKOs and Neurod6-Shh cKOs as judged by Ki67 (a decease by 35±3% and 27±2%, respectively, Figure 7g, h, j, in relation to the control) and Tbr2 (a decrease by 60±7% and 38±4%, respectively, Figure S5f–i, j, in relation to the control). Consequently, the thickness of the GCL was affected among the different genotypes: about 8 cells in the control, 4 cells in Emx1-Smo cKO and 6 cells in Emx1-Shh cKO or Neurod6-Shh cKO (Figure S5f′–i′). The divergent phenotypes in SGZ formation between Emx1-Smo and Emx1-Shh (or Neurod6-Shh) cKOs further validate the model that the Hh-responding cells retained in the ventral hippocampus of the Emx1-Shh cKO or Neurod6-Shh cKO (but completely absent from the Emx1-Smo cKO) are responsible for the initial formation of the SGZ, whereas Shh from the Emx1 domain is relatively dispensable for this in light of the only slightly compromised SGZ in its absence.

As we showed previously that *de novo* local Hh-responding activity was mostly abolished in the Neurod6-Shh cKO (Figure 6e, h, and Figure S3l, l′), we asked in the same genetic background whether Hh-responding cells from the ventral hippocampus can contribute to dorsal dentate development, in particular, SGZ formation, by genetic fate-mapping analysis with the Gli1-CreERT2 line. For that purpose, we examined animals by P15 with tamoxifen injection at birth using Ai14 as the cre reporter. We confirmed that Neurod6-cre showed recombination activity mostly in the outer GCL with little in the inner GCL (Figure 7k, k′) but not in the SGZ at all (Figure 7k″) (Goebbels et al., 2006). In $Gli1^{creERT2/+};Ai14^{F/+};Shh^{F/F}$ animals, tdT+ cells occupied both the inner GCL and SGZ, as indicated by colabeling with the stem cell marker Sox2 (Figure 7l, l′ and l″). Strikingly, in $Gli1^{creERT2/+};Neurod6^{cre/+};Ai14^{F/+};Shh^{F/F}$ animals, tdT+ cells not only populated the outer GCL but also in the inner GCL (Figure 7m, m′) with a few co-expressing Sox2 in the SGZ (arrows in the Figure 7m″). These data taken together indicate that even in the absence of local Shh in the forming DG, descendants of Hh-responding cells in the ventral hippocampus still contribute to the GCL and a few of them also take up residence in the SGZ, whereas in the presence of local Shh, more descendants can be retained in the SGZ, supporting the idea that the local Shh serves to maintain NSCs in the SGZ.

The descendants of the prenatal Hh-responding cells contribute to the LL-NSCs in the SGZ

The long-term fate of the descendants derived from the prenatal Hh-responding cells hasn't been determined yet. By crossing the Gli1-CreERT2 line with the cre reporter Ai14, we could evaluate the tdT expressing cells over a long time after tamoxifen injection at E17.5. In order to increase neurogenesis in aging animals (van Praag et al., 2000), we also subjected them to environment enrichment (EE) for two months and then examined the SGZ when they reached one-year of age (Figure 8a). A number of radially oriented tdT+ cells still retained the expression of the radial glia marker Blbp (arrows in Figure 8b, c). More importantly, some of the tdT+ cells also expressed the immature neuronal marker Dcx (arrows in Figure 8d, e). Therefore, some of the descendents derived from the prenatatal Hh-responding cells maintain the characteristics of NSCs and they are still neurogenic even in aged animals.

DISCUSSION

Since the discovery of neurogenesis in the adult rodent hippocampus (Altman and Das, 1967), the central question of where and how the LL-NSCs relocate to the SGZ of the DG has remained unresolved. Identification of the embryonic origin of the LL-NSCs is the first and perhaps the most important step toward a thorough understanding of this complex developmental process. It has been assumed in the literature that the resident NSCs in the SGZ come from the dentate primordium/VZ at the equivalent longitudinal level (Altman and Bayer, 1990a; Eckenhoff and Rakic, 1984; Li and Pleasure, 2005). In this study, we provide evidence that NSCs from the ventral hippocampus contribute to the development of the SGZ throughout the longitudinal axis of the hippocampus. Moreover, the analysis of the interaction between Hh-responding and Hh-producing cells in the perinatal and postnatal DG not only lends extra support for this model but also reveals the distinct roles of Shh from the different sources in SGZ formation and maintenance.

The ventral hippocampus contributes to the neural stem cells in the subgranular zone

How to keep track of the long-term behaviors of the embryonic NSCs is the main challenge in studying the embryonic origins of adult LL-NSCs. First of all, the markers (such as Nestin, Gfap, Blbp, Glast, etc.) commonly used to label embryonic NSCs may not reliably predict their future fates, since embryonic NSCs can lose their “stemness” due to proliferation/differentiation during development; secondly, it is still hard to predict cell fates by simply referring to their initial anatomical locations, since there is a drastic reorganization during the development of the dentate gyrus; thirdly, the relatively long developmental process to establish the SGZ makes time-lapse imaging techniques impractical. In light of these technical considerations, inducible genetic fate mapping tools are the most powerful way to address this issue (Joyner and Zervas, 2006). Examining the genetically tagged progeny of embryonic NSCs opens up the possibility of following the temporal lineage allocation and teasing out the temporal contribution of embryonic NSCs of distinct origins to adult hippocampal LL-NSCs in the SGZ.

Our static analysis of the developing hippocampus showed the predominant localization of Gli1-nLacZ+ Hh-responding cells in the VZ of the amygdalo-hipppocampal area during late gestation and a gradient of Gli1-nLacZ+ cells in the temporo-septal direction at perinatal ages, providing the first hint that embryonic NSCs in the ventral hippocampus may be the potential source for the LL-NSCs in the SGZ of the dorsal DG. This notion is further strengthened by our fate-mapping analysis. At E17.5, most Hh-responding cells were still restricted to the ventral hippocampus, the progeny of which could be genetically marked with the Gli1-CreERT2 upon tamoxifen induction; these cells were later found in the postnatal SGZ at all septotemporal levels. *de novo* Hh-responding cells also gradually appeared locally in the hilus of the dorsal hippocampus postnatally; however, the progeny of the Hh-responding cells derived from the ventral hippocampus appeared at more septal levels along the longitudinal axis in the dorsal DG before the local Hh-responding cells were detected. The functional significance of the ventral hippocampus-derived NSCs is further established by the regional manipulations of Shh signaling. In addition to confirming that Hh-signaling is essential for the development of the NSCs in the SGZ (Han et al., 2008; Machold et al., 2003), the SGZ deficiency in the Emx1-Smo cKOs directly supports the notion that SGZ NSCs arise exclusively from the Emx1 domain. When Shh was removed from the entire Emx1 domain, local Hh-responding cells in the DG were abolished in the whole hippocampus whereas the Hh-responding cells in the VZ of the ventral hippocampus were relatively unaffected. Thus, the relative intactness of the SGZ in the dorsal hippocampus of Emx1-Shh cKOs can only be accounted for by the Hh-responding cells retained in the ventral hippocampus, which appear sufficient to serve as the source for the NSCs of the SGZ in the dorsal hippocampus. Indeed, genetic fate-mapping analysis with

Gli1-CreERT2 line in the Neurod6-Shh cKO background demonstrated that descendants of the Hh-responding cells from the perinatal age can contribute to the inner granule cell layer and NSCs in the SGZ by P15 even in the absence of the *de novo* local Hh-respsonding activity in the DG. We conclude from these different lines of genetic evidence that embryonic NSCs from the ventral hippocampus contribute to the LL-NSCs in the DG throughout the longitudinal axis of the hippocampus.

The functional significance of this "mosaic" organization of the dentate gyrus with regards to the distinct involvement of the dorsal and ventral dentate in spatial learning vs emotional processing is quite interesting to consider. At this point our data doesn't allow hard conclusions to be drawn regarding the nature of this developmental relationship, however, our elucidation of the developmental origin for the LL-NSC in the dentate is important. In the future, using selective reagents that target ventrally derived LL-NSC selectively should allow novel insights into the circuit and functional relationship between these two divisions of the dentate.

Shh sources for the perinatal and postnatal dentate gyrus

Previous studies suggested that a Shh source from the septum via the septohippocampal projection regulates both SGZ establishment (Machold et al., 2003) and maintenance (Lai et al., 2003). Our analysis of Hh-responding cells with Gli1-nLacZ line in the Emx1-Shh cKO background shows that Shh from pallial sources is exclusively responsible for all the Hh-responding activity in the hippocampus throughout the septotemporal axis, except the VZ of the ventral hippocampus. The new findings in this study argue against the direct contribution of Shh from the septum. Shh was also suggested to be a target gene of Sox2 in the DG NSCs, and thus NSCs are proposed to be the Shh source for the feedback regulation (Favaro et al., 2009). However, our cumulative fate-mapping analysis with the Shh-gfpcre doesn't seem to mark any NSCs in the DG and more importantly, removal of Shh from the differentiated neuronal lineage by Neurod6-cre is sufficient to abolish literally all the Hh-responding activity in the DG, supporting the idea that Shh involved in the regulation of adult SGZ mainly comes from neurons rather than other local cell types (either astrocytes or progenitors).

Relationship between the mediolateral and temporoseptal migratory streams during dentate development

Previous studies revealed the successive development of germinative matrices at different locations during the formation of the DG (Altman and Bayer, 1990a, b). Around the beginning of the third week of gestation in mice, the primary matrix is noticeable at the VZ of the dentate primordium, whereas the secondary matrix develops in the SVZ of the dentate primordium throughout the third week of gestation (Li et al., 2009). At perinatal ages, the secondary matrix dissolves into two components (Altman and Bayer, 1990a), the extrinsic component extends subpially and forms the transient neurogenic niche that gives rise to the outer shell of the GCL (Li et al., 2009), whereas the intrinsic component invades the hilus and gives rise to the tertiary matrix (Altman and Bayer, 1990a). During the second postnatal week, the tertiary matrix progressively gives way to the SGZ (Altman and Bayer, 1990a; Li et al., 2009). In addition to this well-recognized stream originating from the VZ of the dentate at the equivalent longitudinal level, which migrates in the mediolateral direction, in this study we provide evidence for the presence of another stream, originating from the VZ of the ventral hippocampus and spreading in the temporoseptal direction (red arrow in Figure 3j). These two different streams appear to converge at the entrance of the hilus in close proximity to the pial meninges. In the Emx1-Smo cKO, the extrinsic component (the subpial component) is only moderately affected, whereas the intrinsic component is severely compromised, supporting the idea that the mediolateral migratory stream is Hh-independent

and mainly contributes to development of the outer shell of the suprapyramidal blade, while the temporoseptal migratory stream originating from the ventral hippocampus is Hh-dependent and mostly contributes to the development of the tertiary matrix, the inner shell of the DG and the prospective SGZ.

Previous work using minimal aggregation chimeras indicated that the outer portion of the dentate granule cell layer had a developmentally divergent origin from the bulk of the granule neurons residing in the inner portion of the granule cell layer, which are believed to arise from SGZ progenitors (Martin et al., 2002). In this assay, it is difficult to dissect when and where the chimeric LacZ aggregates came from at the anatomical level. Our genetic fate-mapping analysis using the Gli1-CreERT2 line with tamoxifen induction shows that the inner and outer portions of the dentate have distinct but somewhat overlapping temporal origins between E15.5 and P0. As well, our identification of the ventral source of the LL-NSCs further supplies an anatomic distinction between the birth of embryonically produced DGC at widespread septotemporal levels while providing evidence for a distinct anatomic origin for the SGZ NSCs.

In summary, we have provided new evidence linking the developmental origin of the LL-NSCs in the adult dentate gyrus to the germinative VZ in the ventral hippocampus. We believe this new finding will lead to a new framework to understand the general paradigms for retaining the LL-NSCs in the different anatomical structures in the adult brain.

EXPERIMENTAL PROCEDURES

Animals

The following mouse lines were obtained from Jackson Laboratory (Bar Harbor, ME): Gli1-nLacZ (stock#008211), Gli1-CreERT2 (stock#007913), Ai14 (stock#007914), Rosa-Yfp (stock#006148), Emx1-cre (stock#05628), Nes-Cre (stock#003771), Shh-gfpcre (stock#005622), Shh-CreERT2 (stock#005623), $Shh^{flox/flox}$ (stock#004293), $Smo^{flox/flox}$ (stock#004526). Olig2-cre is kindly provided by Dr. D. Rowitch (UCSF) and Neurod6-Cre by Drs. S. Goebbels and K.A. Nave (Max Planck). The day of vaginal plug was considered embryonic day 0.5 (E0.5). Mouse colonies were maintained at UCSF in accordance with National Institutes of Health and UCSF guidelines.

Environment Enrichment (EE)

For environment enrichment, 6–10 mice were housed in the One Cage 2100 system, which is almost triple the size of the regular cage. The cages were also equipped with igloos, tunnels, running wheels and various toys.

Tamoxifen induction

Tamoxifen (T5648, Sigma) was dissolved in corn oil (C8267, Sigma) at 20mg/ml. Pregnant females were administrated intraperitoneally (I.P.) with 3mg of tamoxifen per 40g animal. Neonates were injected subcutaneously with 50ul of tamoxifen stock solution.

LacZ staining

Animals for LacZ staining were perfused with 2% paraformaldehyde (PFA) and the dissected brains were postfixed with 2% PFA for 2hrs at 4°C. Tissues were cryoprotected in 30% sucrose, embedded in OCT and then kept at −80°C for long-ter m storage. Perinatal tissues were sectioned at 20μm and P7 tissues at 16μm. X-gal staining was developed at 37°C overnight in the staining solution [5mM $K_3Fe(CN)_6$, 5mM $K_4Fe(CN)_6$, 5mM EGTA, 0.01% deoxycholate, 0.02% NP40, 2mM $MgC1_2$, 1mg/ml X-gal]. Sections were post-fixed with 10% formalin at room temperature overnight. Slides were then counterstained with

nuclear-fast red (H-3403, Vector Laboratories) at room temperature for 10min before proceeding for dehydration (70%, 95%, 100% ethanol, xylene twice) and coverslipping with Mount-Quick (Ted Pella).

Immunohistochemistry

Animals were perfused with 1xPBS followed by 4% PFA. Dissected brains were post-fixed in 4% PFA overnight. They were then cryoprotected in 30% sucrose until they sank. Brain tissues were embedded in OCT and kept at −80°C. Brain secti ons made on a cryostat at 12μm were directly collected on slides for perinatal tissues, or cut at 30μm for P15 or older tissues as floating sections in 1xPBS and mounted onto slides after staining. Sections were stained with the following primary antibodies overnight at 4°C i n blocking buffer (10% lamb serum, 0.3% Triton X-100, 0.05% NaN_3 in 1xPBS); then rinsed in wash buffer (0.3%Triton X-100 in 1xPBS) three times. They were further stained with the Alexa fluorochrome-conjugated secondary antibodies (Invitrogen) in the same blocking buffer for 2hrs at room temperature and counter stained with DAPI for 0.5hr. Primary antibodies were used as followed: rat anti-GFP (1:1,000; Nacalai Tesque), rat anti-Ctip2 (1:1000; Abcam), rabbit anti-Blbp (1:1,000; Chemicon), rabbit anti-Calretinin (1:1000; Chemicon), rabbit anti-Ki67 (1:500, monoclonal antibody; Neomarker), rabbit anti-Tbr2 (1:1,000; gift from Dr. R. Hevner, University of Washington, Seattle), rabbit anti-Gfap (1:1,000; Dako), rabbit anti-Laminin (1:500; Sigma-Aldrich), rabbit anti-Otp (1:1,000; gift from Dr. F. Vaccarino, Yale University), guinea pig anti-Sox10 (1:1,000; gift from Dr. M. Wegner, Institut für Biochemie, Germany), rabbit anti-Olig2 (1:1,000; gift from Dr. D. Rowitch, UCSF), rabbit anti-Dcx (1:500; Abcam), rabbit anti-Sox2 (1:1,000; Epitomics).

Image analysis and quantification

Images were acquired using a Nikon E600 microscope equipped with a cooled-CCD camera (QCapture Pro; QImaging, Burnaby, British Columbia, Canada). For colocalization analysis, confocal images were taken with LSM 510 meta two-photon microscope (Carl Zeiss, Inc.). Brain sections of the similar anatomical levels from five brains for controls or mutants were chosen for quantification. The densities of indicated cell types in each region were quantified and shown as percentage of the mean ± standard error of the mean (SEM) for N given samples over the controls. Data were analyzed using two-tailed Student's *t*-test with unequal variance. Any p-value less than 0.05 was considered significant.

Supplementary Material

Refer to Web version on PubMed Central for supplementary material.

Acknowledgments

We thank Drs. J.L.R. Rubenstein, A. Chen, G. Beaudoin and Y. Wang for comments on the manuscript, T. Huynh, Y. Choe and other members in the Pleasure's lab for the technical assistance. This work was supported by NIH Grant R01 MH077694 and gift funding from the family of Glenn W. Johnson, Jr.

References

Ahn S, Joyner AL. Dynamic changes in the response of cells to positive hedgehog signaling during mouse limb patterning. Cell. 2004; 118:505–516. [PubMed: 15315762]

Ahn S, Joyner AL. In vivo analysis of quiescent adult neural stem cells responding to Sonic hedgehog. Nature. 2005; 437:894–897. [PubMed: 16208373]

Altman J, Bayer SA. Migration and distribution of two populations of hippocampal granule cell precursors during the perinatal and postnatal periods. J Comp Neurol. 1990a; 301:365–381. [PubMed: 2262596]

Altman J, Bayer SA. Mosaic organization of the hippocampal neuroepithelium and the multiple germinal sources of dentate granule cells. J Comp Neurol. 1990b; 301:325–342. [PubMed: 2262594]

Altman J, Das GD. Postnatal neurogenesis in the guinea-pig. Nature. 1967; 214:1098–1101. [PubMed: 6053066]

Bai CB, Auerbach W, Lee JS, Stephen D, Joyner AL. Gli2, but not Gli1, is required for initial Shh signaling and ectopic activation of the Shh pathway. Development. 2002; 129:4753–4761. [PubMed: 12361967]

Breunig JJ, Sarkisian MR, Arellano JI, Morozov YM, Ayoub AE, Sojitra S, Wang B, Flavell RA, Rakic P, Town T. Primary cilia regulate hippocampal neurogenesis by mediating sonic hedgehog signaling. Proc Natl Acad Sci U S A. 2008; 105:13127–13132. [PubMed: 18728187]

Clelland CD, Choi M, Romberg C, Clemenson GD Jr, Fragniere A, Tyers P, Jessberger S, Saksida LM, Barker RA, Gage FH, et al. A functional role for adult hippocampal neurogenesis in spatial pattern separation. Science. 2009; 325:210–213. [PubMed: 19590004]

Eckenhoff MF, Rakic P. Radial organization of the hippocampal dentate gyrus: a Golgi, ultrastructural, and immunocytochemical analysis in the developing rhesus monkey. J Comp Neurol. 1984; 223:1–21. [PubMed: 6707248]

Encinas JM, Michurina TV, Peunova N, Park JH, Tordo J, Peterson DA, Fishell G, Koulakov A, Enikolopov G. Division-coupled astrocytic differentiation and age-related depletion of neural stem cells in the adult hippocampus. Cell Stem Cell. 2011; 8:566–579. [PubMed: 21549330]

Favaro R, Valotta M, Ferri AL, Latorre E, Mariani J, Giachino C, Lancini C, Tosetti V, Ottolenghi S, Taylor V, et al. Hippocampal development and neural stem cell maintenance require Sox2-dependent regulation of Shh. Nat Neurosci. 2009

Galceran J, Miyashita-Lin EM, Devaney E, Rubenstein JL, Grosschedl R. Hippocampus development and generation of dentate gyrus granule cells is regulated by LEF1. Development. 2000; 127:469–482. [PubMed: 10631168]

Garcia AD, Petrova R, Eng L, Joyner AL. Sonic hedgehog regulates discrete populations of astrocytes in the adult mouse forebrain. J Neurosci. 2010; 30:13597–13608. [PubMed: 20943901]

Goebbels S, Bormuth I, Bode U, Hermanson O, Schwab MH, Nave KA. Genetic targeting of principal neurons in neocortex and hippocampus of NEX-Cre mice. Genesis. 2006; 44:611–621. [PubMed: 17146780]

Han YG, Spassky N, Romaguera-Ros M, Garcia-Verdugo JM, Aguilar A, Schneider-Maunoury S, Alvarez-Buylla A. Hedgehog signaling and primary cilia are required for the formation of adult neural stem cells. Nat Neurosci. 2008; 11:277–284. [PubMed: 18297065]

Harfe BD, Scherz PJ, Nissim S, Tian H, McMahon AP, Tabin CJ. Evidence for an expansion-based temporal Shh gradient in specifying vertebrate digit identities. Cell. 2004; 118:517–528. [PubMed: 15315763]

Joyner AL, Zervas M. Genetic inducible fate mapping in mouse: establishing genetic lineages and defining genetic neuroanatomy in the nervous system. Dev Dyn. 2006; 235:2376–2385. [PubMed: 16871622]

Lai K, Kaspar BK, Gage FH, Schaffer DV. Sonic hedgehog regulates adult neural progenitor proliferation in vitro and in vivo. Nat Neurosci. 2003; 6:21–27. [PubMed: 12469128]

Li G, Berger O, Han SM, Paredes M, Wu NC, Pleasure SJ. Hilar mossy cells share developmental influences with dentate granule neurons. Dev Neurosci. 2008; 30:255–261. [PubMed: 17960053]

Li G, Kataoka H, Coughlin SR, Pleasure SJ. Identification of a transient subpial neurogenic zone in the developing dentate gyrus and its regulation by Cxcl12 and reelin signaling. Development. 2009; 136:327–335. [PubMed: 19103804]

Li G, Pleasure SJ. Morphogenesis of the dentate gyrus: what we are learning from mouse mutants. Dev Neurosci. 2005; 27:93–99. [PubMed: 16046842]

Li G, Pleasure SJ. Ongoing interplay between the neural network and neurogenesis in the adult hippocampus. Curr Opin Neurobiol. 2010; 20:126–133. [PubMed: 20079627]

Machold R, Hayashi S, Rutlin M, Muzumdar MD, Nery S, Corbin JG, Gritli-Linde A, Dellovade T, Porter JA, Rubin LL, et al. Sonic hedgehog is required for progenitor cell maintenance in telencephalic stem cell niches. Neuron. 2003; 39:937–950. [PubMed: 12971894]

Machon O, Backman M, Machonova O, Kozmik Z, Vacik T, Andersen L, Krauss S. A dynamic gradient of Wnt signaling controls initiation of neurogenesis in the mammalian cortex and cellular specification in the hippocampus. Dev Biol. 2007; 311:223–237. [PubMed: 17916349]

Madisen L, Zwingman TA, Sunkin SM, Oh SW, Zariwala HA, Gu H, Ng LL, Palmiter RD, Hawrylycz MJ, Jones AR, et al. A robust and high-throughput Cre reporting and characterization system for the whole mouse brain. Nat Neurosci. 2010; 13:133–140. [PubMed: 20023653]

Mangale VS, Hirokawa KE, Satyaki PR, Gokulchandran N, Chikbire S, Subramanian L, Shetty AS, Martynoga B, Paul J, Mai MV, et al. Lhx2 selector activity specifies cortical identity and suppresses hippocampal organizer fate. Science. 2008; 319:304–309. [PubMed: 18202285]

Martin LA, Tan SS, Goldowitz D. Clonal architecture of the mouse hippocampus. J Neurosci. 2002; 22:3520–3530. [PubMed: 11978829]

Sahay A, Scobie KN, Hill AS, O'Carroll CM, Kheirbek MA, Burghardt NS, Fenton AA, Dranovsky A, Hen R. Increasing adult hippocampal neurogenesis is sufficient to improve pattern separation. Nature. 2011

Schuller U, Heine VM, Mao J, Kho AT, Dillon AK, Han YG, Huillard E, Sun T, Ligon AH, Qian Y, et al. Acquisition of granule neuron precursor identity is a critical determinant of progenitor cell competence to form Shh-induced medulloblastoma. Cancer Cell. 2008; 14:123–134. [PubMed: 18691547]

Super H, Soriano E. The organization of the embryonic and early postnatal murine hippocampus. II. Development of entorhinal, commissural, and septal connections studied with the lipophilic tracer DiI. J Comp Neurol. 1994; 344:101–120. [PubMed: 8063952]

van Praag H, Kempermann G, Gage FH. Neural consequences of environmental enrichment. Nat Rev Neurosci. 2000; 1:191–198. [PubMed: 11257907]

Zhou CJ, Zhao C, Pleasure SJ. Wnt signaling mutants have decreased dentate granule cell production and radial glial scaffolding abnormalities. J Neurosci. 2004; 24:121–126. [PubMed: 14715945]

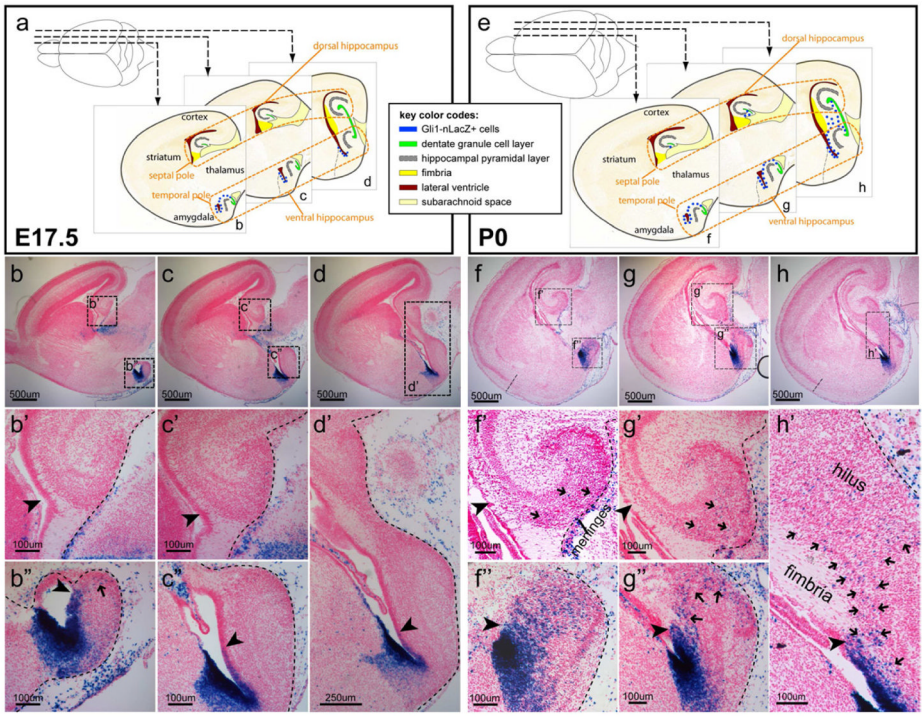

Figure 1. Perinatal distribution of Gli1-nLacZ Hh-responding cells in the hippocampus

(**a**) Schemas of Gli1-nLacZ distribution at E17.5 were shown at the three levels of the sagittal sections.

(**b-d**) From medial to lateral, three levels of sagittal sections for Gli1-nLacZ staining at E17.5 were shown. At E17.5, Gli1-nLacZ expression occupied the whole ventricular zone (VZ) of the ventral hippocampus at the far end of the temporal pole (**b″** arrowhead), half at the mid-level (**c″** arrowhead), but only one-third at the transitional level (**d′** arrowhead). A stream of Gli1-nLacZ+ cells from VZ to the dentate pole were noticeable at the end of the temporal pole (**b″** arrow). Gli1-nLacZ+ cells were clearly absent in the dorsal dentate primordium (**b′, c′** arrowheads). (**e**) Schemas of Gli1-nLacZ distribution at P0 were shown at the three levels of the sagittal sections.

(**f–h**) From medial to lateral, three levels of sagittal sections for Gli1-nLacZ staining at P0 were shown. At P0, Gli1-nLacZ expression covered the whole VZ of the ventral hippocampus at all levels (**f″**, **g″** and **h′** arrowheads). By contrast, Gli1-nLacZ remained absent from the dentate primordium in the dorsal hippocampus (**f′** and **g′** arrowheads). At the transitional level, Gli1-nLacZ+ cells spread from ventral to dorsal (**h′** arrows). Sparse Gli1-nLacZ+ cells were also detected in the dorsal DG displaying a gradient with the lowest in the septal pole (**f′, g′** and **h′** arrows).

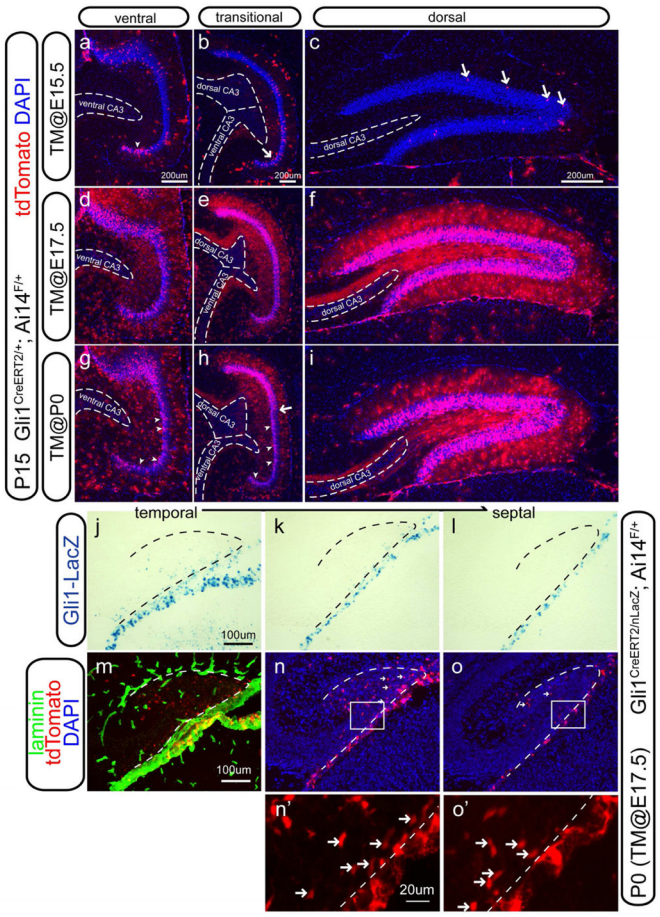

Figure 2. Fate-mapping analysis of Hh-responding cells by Gli1-CreERT2 with prenatal or perinatal tamoxifen injections

(**a**–**i**) The distribution of tdT+ cells in the dentate gyrus was examined at P15 in mice carrying both Gli1-CreERT2 and Cre reporter Ai14 after tamoxifen (TM) injection at E15.5 (**a**–**c**), E17.5 (**d**–**f**) and P0 (**g**–**i**), of which the ventral (**a**, **d**, **g**), transitional (**b**, **e**, **h**) and dorsal (**c**, **f**, **i**) aspects were shown respectively.

(**j**–**o**) Mice carrying Gli1CreERT2, Gli1-nLacZ and Ai14 were analyzed at P0 after tamoxifen injection at E17.5. At P0, the representative sagittal sections of the dorsal DG from temporal (**j**) to septal (**l**) levels were shown for Gli1-nLacZ distribution. In the meantime, the distributions of tdT+ cells representing the progeny of the recombined cells were shown with the next sections corresponding to (**j**–**k**). The complete set of the alternative sections for the Gli1-nLacZ and tdT+ cells were shown in the Figure S1. Basement membrane of the meninges and blood vessels were labeled by Laminin expression (**m**). Of note, tdT+ cells were detectable at the septal level (arrows in **n** and **o**) where Gli1-nLacZ expression was absent in the dentate field (**k** and **l**). Boxed areas in Figure 2n and Figure 2o were shown at the higher magnification in Figure 2n′ and Figure 2o′, the arrows in which highlighted the presence of tdT+ cells at the entrance of the hilus.

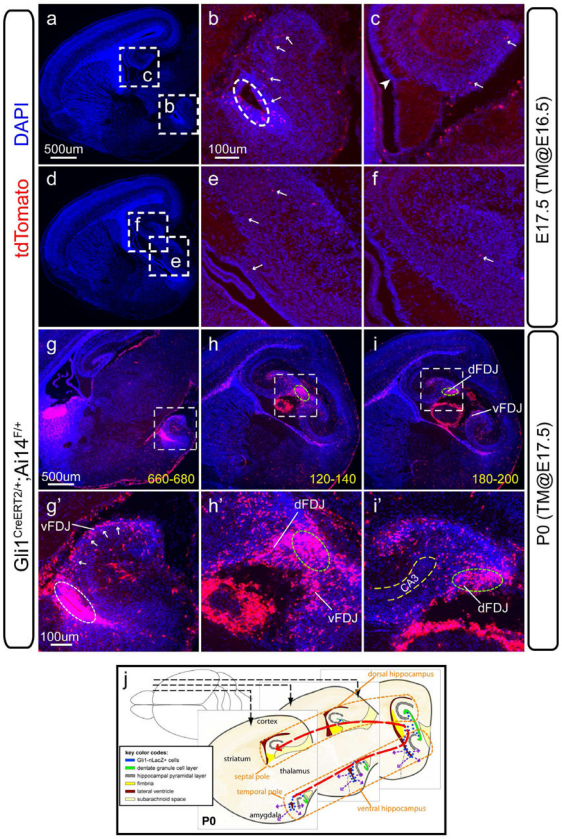

Figure 3. The short-term distribution for the progeny of Hh-responding cells derived from the ventral hippocampus

(**a**–**f**) The distribution of tdT+ cells in the Gli1$^{CreERT2/+}$;Ai14$^{F/+}$ animals were shown one day after tamoxifen (TM) induction at E16.5. The two representative sagittal levels (**a** and **d**) were used for analysis. Boxed areas were shown at the higher magnification in **b, c, e** and **f**. From the temporal pole to the septal pole, the tdT+ cells (arrows in **b**, **e**, **f** and **c**) displayed a gradient distribution.

(**g**–**i**) The distribution of tdT+ cells in the Gli1$^{CreERT2/+}$;Ai14$^{F/+}$ animals were shown two day after tamoxifen (TM) induction at E17.5. The three representative sagittal sections were chosen to highlight the main features of the tdT+ cells from the newborns (P0), whereas a series of sections from every 60μm were shown in the Figure S2. The progeny of Hh-responding cells were identified by tdT expression. Throughout the whole hippocampus, the VZ of the temporal hippocampus was the most heavily labeled by tdT (white oval in **g′**). There was a remarkable cell stream in the vFDJ regions (arrows in **g′**). The tdT+ cells were continuous from the vFDJ into the dFDJ at the transitional level (green oval in **h** and **h′**) and tapered off in the dorsal hippocampus toward the septal pole (green oval in **i** and **i′**). The thickness distance as micron from the first section (in the Figure S2.) was shown at the bottom-right corners in **g**, **h** and **i**. dFDJ, dorsal fimbriodentate junction; vFDJ, ventral fimbriodentate junction.

(**j**) The schema shows the temporal-to-septal distribution (red arrow) of the progeny of the Hh-responding cells originated from the VZ of the ventral hippocampus at the perinatal age. In addition, the VZ of the amygdalo-hippocampal region also gives rise to other cells in different directions (purple arrows).

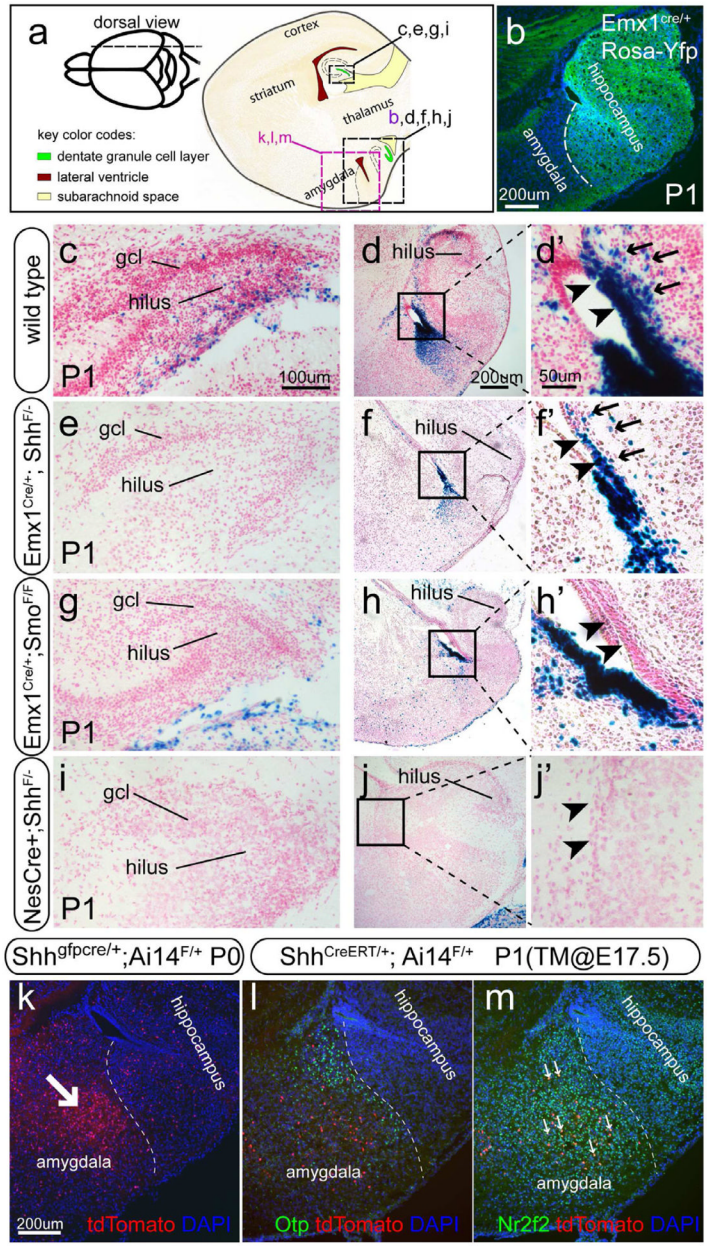

Figure 4. Perinatal distribution of Gli1-nLacZ in various Shh signaling conditional mutants

(**a**) The schemas are illustrated for the sagittal sections from the P1 animals shown in **b**–**m**.

(**b**) With the cre reporter Rosa-Yfp, Emx1-cre showed recombination in the ventral hippocampus.

(**c**, **d** and **d′**) In the control, Gli1-nLacZ+ cells were detected in the hilus of both dorsal (**c**) and ventral (**d**) DG, and particularly in the VZ of the ventral hippocampus (arrowheads in **d′**). Gli1-nLacZ+ cells were obvious in the region away from the VZ (arrows in **d′**).

(**e**, **f** and **f′**) In the Emx1-Shh conditional knockout, Gli1-nLacZ+ cells were absent from the hilus of both dorsal and ventral DG (**e**, **f**) but still present in the VZ of the ventral hippocampus (**f′**). Gli1-nLacZ+ cells were still evident in the region away from the VZ (arrows in **f′**).

(**g**, **h** and **h′**) In the Emx1-Smo conditional knockout, Gli1-nLacZ+ cells were absent in the dorsal (**g**) and ventral hippocampus (**h** and arrowheads in **h′**) without affecting their distribution in the VZ of the amygdala (**h**, **h′**).
(**i**, **j** and **j′**) In the NesCre-Shh conditional knockout, Gli1-nLacZ activity was completely abolished in the hippocampus and the VZ of the amygdalo-hippocampal region.
(**k**–**m**) A domain of Shh-producing cells was located in the amygdala. At P0, cumulative fate-mapping with the Shh-gfpcre and Ai14 lines showed a tdT+ domain in the amygdala (arrow in **k**). The fate-mapping analysis with Shh-CreERT2 and Ai14 upon tamoxifen injection at E17.5, showed a subset of tdT+ cells at P1 in the amygdala as in (**k**). They were co-labeled with Nr2f2 (arrows in **m**) but not overlapped with the Otp+ cells (**l**).

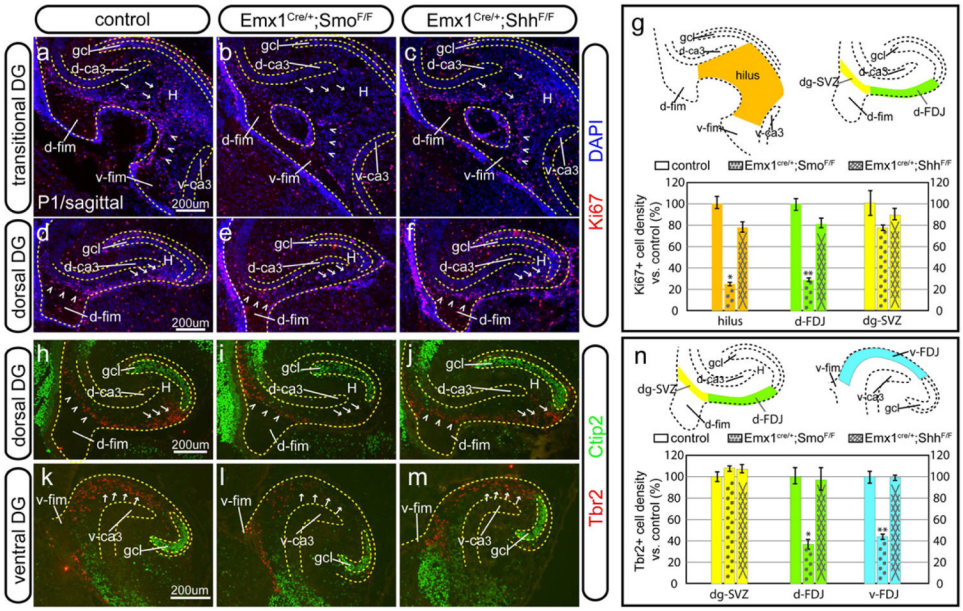

Figure 5. The dentate migratory streams in the Shh signaling conditional mutants

(**a**–**f**) Ki67+ proliferative cells at P1 were shown at the transitional level (**a**–**c**) and in the dorsal DG (**d**–**f**) for the control (**a**, **d**), Emx1-Smo cKO (**b**, **e**) and Emx1-Shh cKO (**c**, **f**), respectively. Compared to the control, Ki67+ proliferating cells in both the hilar region (arrows in **a**–**c**) and the hilar entrance from the ventral hippocampus (arrowheads in **a**–**c**) were severely compromised in the Emx1-Smo cKO but only mildly affected in the Emx1-Shh cKO. In the dorsal hippocampus, they showed comparative number of Ki67+ cells at the SVZ of the dentate primordium (arrowheads in **d**–**f**). However, compared to the control (arrows in **d**), Ki67+ cells in the dFDJ were greatly diminished in the Emx1-Smo cKO (arrows in **e**) but only slightly reduced in the Emx1-Shh cKO (arrows in **f**).

(**g**) Quantification is shown for the density of Ki67+ cells in various regions from the control, Emx1-Smo cKO and Emx1-Shh cKO. Compared to the control (100±6% and 100±6%), the Ki67+ cell densities found in the hilus (orange) and d-FDJ (green) were only 25±2% (n=5, p<0.001) and 29±2% (n=5, p<0.001) for the Emx1-Smo cKO, whereas they were 78±5% (n=5, p<0.05) and 81±5% (n=5, p<0.05) for the Emx1-Shh cKO. In the dg-SVZ (yellow), the Ki67+ cell densities in the Emx1-Smo cKOs and Emx1-Shh cKOs were 77±3% (n=5, p= 0.13) and 89±6% (n=5, p=0.42) as much as the controls (100±12%).

(**h**–**m**) Tbr2+ neurogenic cells at P1 were shown in the dorsal DG (**h**–**j**) and the ventral DG (**k**–**m**) for the control (**h**, **k**), Emx1-Smo cKO (**i**, **l**) and Emx1-Shh cKO (**j**, **m**), respectively. Similar to the Ki67 pattern, they showed comparative number of Tbr2+ cells at the SVZ of the dentate primordium (arrowheads in **h**–**j**). However, compared to the control (arrows in **h**), Tbr2+ cells in the dFDJ were greatly diminished in the Emx1-Smo cKO (arrows in **i**) but only slightly reduced in the Emx1-Shh cKO (arrows in **j**). In relation to the control (arrows in **k**), Tbr2+ cells in the vFDJ were greatly diminished in the Emx1-Smo cKO (arrows in **l**) but only slightly reduced in the Emx1-Shh cKO (arrows in **m**).

(**n**) Quantification is shown for the density of Tbr2+ cells in various regions from the control, Emx1-Smo cKO and Emx1-Shh cKO. In the dg-SVZ (yellow), Tbr2+ cell densities were comparable among the three genotypes: 100±5% for the control, 108±3% for the Emx1-Smo cKO (n=5, p= 0.39) and 107±4% for Emx1-Shh cKO (n=5, p=0.58). However, compared to the control (100±8% and 100±6%), the Tbr2+ cell densities found in the d-FDJ (green) and v-FDJ (cyan) were 37±3% (n=5, p<0.001) and 45±3% (n=5, p<0.001) for the

Emx1-Smo cKO, whereas they were 97±5% (n=5, p=0.6) and 104±3% (n=5, p=0.14) for the Emx1-Shh cKO.

Data are shown as mean±SEM and p values for the indicated sample sizes were returned by Student's *t*-test for two-tailed distribution with unequal variance.

dg-SVZ, subventricular zone of dentate gyrus; gcl, granule cell layer; d-ca3, dorsal CA3; v-ca3, ventral CA3; H, hilus; d-FDJ, dorsal fimbriodentate junction; v-FDJ, ventral fimbriodentate junction; d-fim, dorsal fimbria; v-fim, ventral fimbria

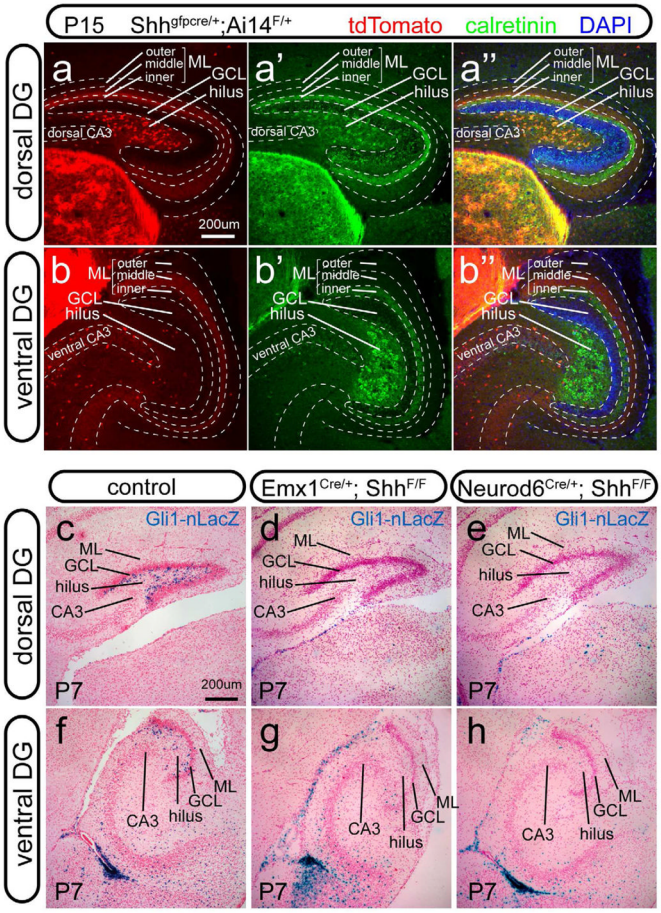

Figure 6. The Shh sources for the postnatal DG

(**a**–**b**) At P15, cumulative fate-mapping of the Shh producing cells with the Shh-gfpcre and Ai14 lines was shown in the dorsal and ventral DG (**a** and **b**, respectively). In the dorsal dentate gyrus, tdT expression was colocalized with hilar mossy cell marker Calretinin (**a′**, **a″**). In the dorsal and ventral dentate gyrus, tdT expression was also detected in the mid-molecular layer (**a″**, **b′**, **b″**) where the neurons of the medial entorhinal cortex project their fibers.

(**c**–**h**) At P7, Gli1-nLacZ+ cells were present in the hilus of both dorsal and ventral DG in the control (**c** and **f**), but completely abolished in the Emx1-Shh cKO (**d** and **g**) and Neurod6-Shh cKO (**e** and **h**).

GCL, granule cell layer; ML, molecular layer; SGZ, subgranular zone.

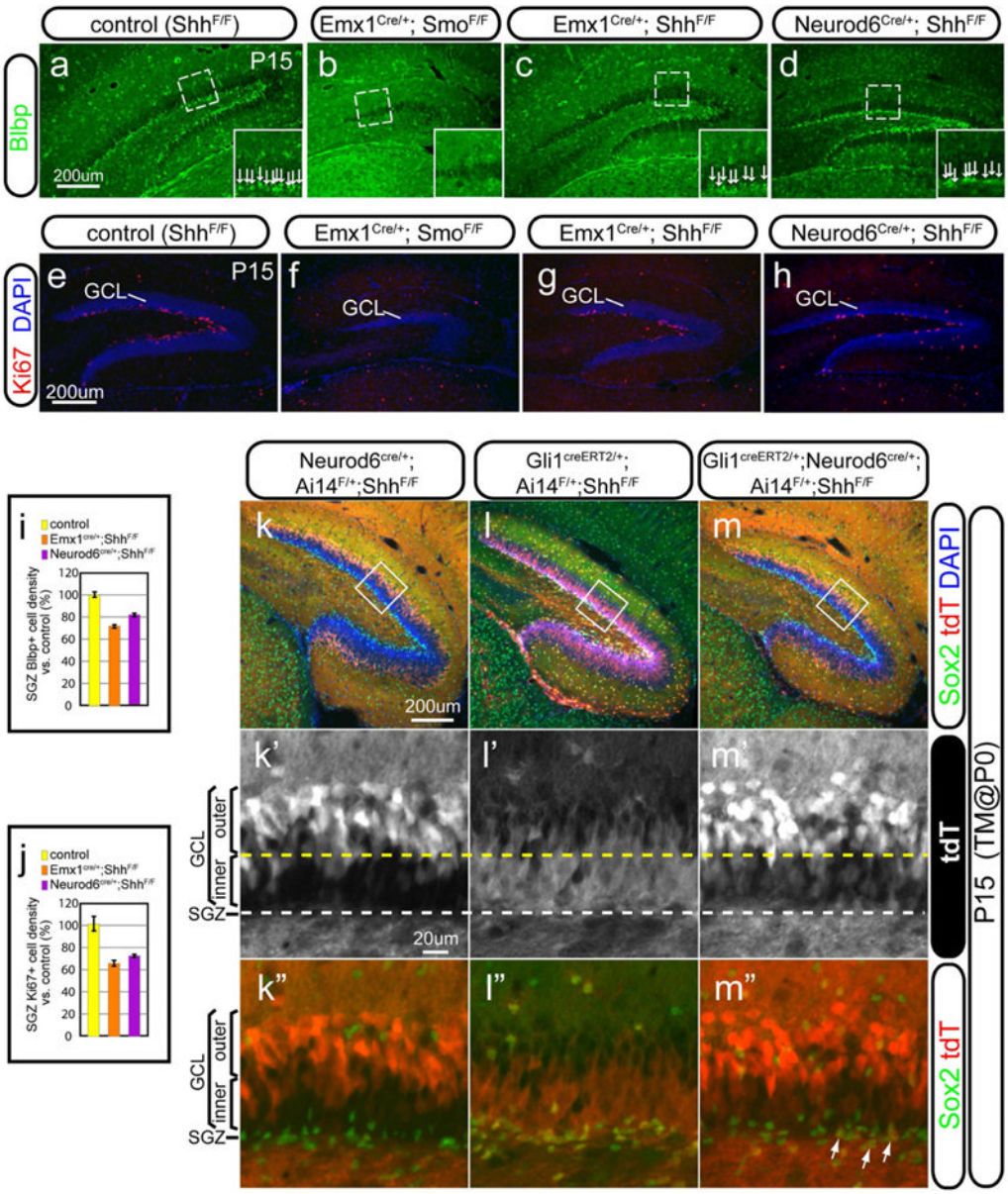

Figure 7. The formation of the SGZ in the Emx1-Smo, Emx1-Shh and Neurod6-Shh cKOs

(**a**–**d**) SGZ formation was assessed with the radia glial marker Blbp in the control (**a**), Emx1-Smo cKO (**b**), Emx1-Shh cKO (**c**) and Neurod6-Shh (**d**). There was a complete lack of Blbp+ cells in the SGZ of Emx1-Smo cKO (**b**) but only a moderate decrease in the Emx1-Shh cKO (**c**) and Neurod6-Shh cKO (**d**). The arrangement of Blbp+ cells in the SGZ was shown at the higher magnification in the insets.

(**e**–**h**) Proliferative Ki67+ cells in the SGZ were shown for the control (**e**), Emx1-Smo cKO (**f**), Emx1-Shh cKO (**g**) and Neurod6-Shh (**h**). Ki67+ cells were completely abolished in the Emx1-Smo cKO (**f**) but only mildly affected in the Emx1-Shh cKO (**k**) and Neurod6-Shh cKO (**d**).

(**i**) Quantification of Blbp+ cell densities in the SGZ was made for the control, Emx1-Shh cKO and Neurod6-Shh cKO. It was 72±4% (n=5, $p<0.01$) in the Emx1-Shh cKOs and 82±3% (n=5, $p<0.01$) in the Neurod6-Shh cKOs, as compared to the controls (100±6%).

(**j**) Quantification of Ki67+ cell densities in the SGZ was made for the control, Emx1-Shh cKO and Neurod6-Shh cKO. It was only 65±3% (n=5, $p<0.01$) in the Emx1-Shh cKOs and 73±2% (n=5, $p<0.01$) in the Neurod6-Shh cKOs, as compared to the controls (100±7%)
(**k**–**m**) Fate-mapping analysis in the absence of local Shh in the DG. Animals were examined by P15 with tamoxifen injection at birth using Ai14 as the cre reporter. In $Neurod6^{cre/+};Ai14^{F/+};Shh^{F/F}$ animals (**k**), tdT+ cells were mostly restricted in the outer GCL (**k′**) but absent from the SGZ as indicated by the lack of colabeling with Sox2, the marker for NSCs (**k″**). In $Gli1^{creERT2/+};Ai14^{F/+};Shh^{F/F}$ animals (**l**), tdT+ cells were present mostly in the inner GCL (**l′**) and SGZ (**l″**). By contrast, in $Gli1^{creERT2/+};Neurod6^{cre/+};Ai14^{F/+};Shh^{F/F}$ animals (**m**), despite the lack of local Shh in the dentate, tdT+ cells were present in both inner GCL (**m′**) and SGZ (arrows in **m″**), in addition to the outer GCL.
Data are shown as mean±SEM and p values for the indicated sample sizes are calculated by Student's *t*-test for two-tailed distribution with unequal variance.
GCL, granule cell layer; SGZ, subgranular zone.

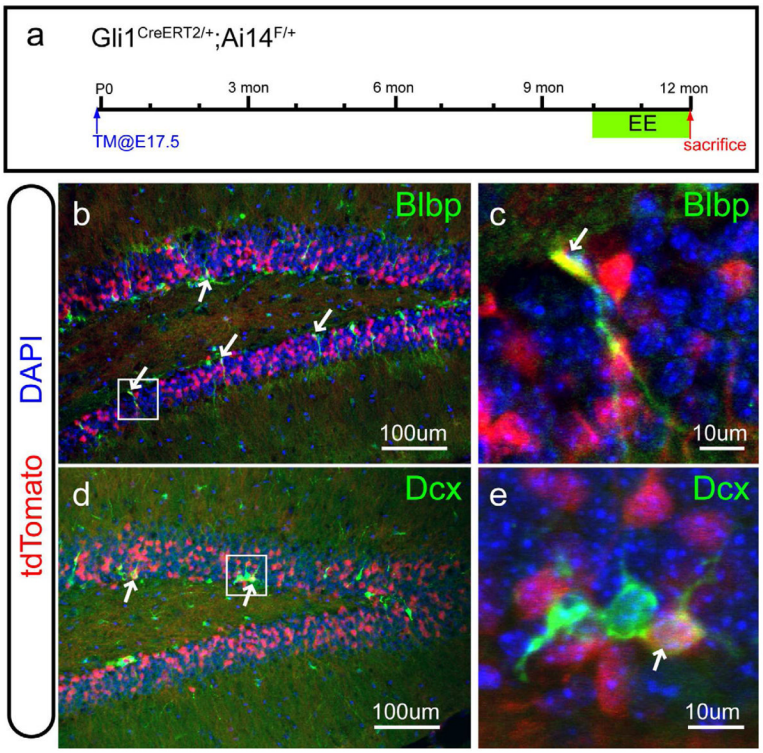

Figure 8. The long-term fate mapping of the prenatal Hh-responding cells in the dentate gyrus

(**a**) The schema shows the strategy for the long-term fate mapping of the prenatal Hh-responding cells in the dentate gyrus. By crossing the Gli1CreERT2 line with the Ai14 line, the cell fate of the Hh-responding cells labeled by tamoxifen injection at E17.5 was examined in the one-year-old animals after environment enrichment (EE) for two months (green box).

(**b**–**c**) Some tdT+ cells were marked by the neural stem cell marker Blbp in the SGZ (arrows in **b**) in the one-year-old animals. The boxed area in (**b**) is shown at the higher magnification in (**c**).

(**d**–**e**) Some tdT+ cells were also labeled by the immature neuronal marker Dcx (arrows in **d**) in the one-year-old animals. The boxed area in (**d**) is also shown at the higher magnification in (**e**).